14

Accurate Axial Location for Particles in Digital In-Line Holography

Zhi-Bin Li[1], Gang Zheng[2], Li-Xin Zhang[2], Gang Liu[1] and Fei Xia[1]
[1]*Shanghai University of Electric Power*
[2]*University of Shanghai for Science and Technology*
China

1. Introduction

The potential of in-line holography to analyze flow by means of particles has been noted since its very beginnings. The development of optical holography applications in fluid mechanics established the capability of holography to provide both particle size and tridimensional position (Adams et al., 2000). In classical holography, the diffraction pattern produced by a particle field is recorded on a holographic plate or film with a collimated laser beam. The reconstruction of the 3D particle images is performed by illuminating developed hologram with the reference beam. In digital holography, the diffraction pattern is directly recorded on a charge-coupled device (CCD) camera and the reconstruction process is performed numerically, plane by plane to produce a region of the reconstructed volume. So the sizes and locations of particles are computed from the reconstructed volume by an automated process.

Recently, this technique has been used to develop a new holographic particle image velocimetry (HPIV) system (Meng et. al., 2004). It is particularly interesting for high-speed phenomena analysis, as in fluid mechanics. But it has become the bottleneck in flow field measurement due to the lower axial positioning accuracy of particle. Many contributions have been made in order to improve the measurement accuracy of the localization of particles. Generally, the two main steps of the numerical processing are a numerical reconstruction step to obtain a synthesized 3D image with focused particles, and a segmentation step to extract locations and sizes of the particles from this 3D distribution.

However, the direct light and twin-images of particles can not be separated from the focused-images of particles in the numerical reconstruction process due to inline optical system, which resulting in the decline in quality for focused-images of particles. The impact of direct light and twin-images of particles can be removed and improved through all kinds of different methods (Kreis et al., 1997 and Takaki et al., 1999)). As an important parameters of imaging system, the depth of focus (DOF) is tens of times or even hundreds of times more than particle diameter in digital in-line Fresnel holographic system (Dubois et al., 2006). However, the DOF of inline digital holographic system is characterized differently in different literatures (Liebling et al., 2004). It is very difficult to give precise expression to DOF of inline digital holographic system. So approximations have to be applied in the analysis of the DOF. DOF is the main reason for the lower axial positioning accuracy of

particle. Because there exists no definitive criterion for finding the focal plane of a scene or finding the focal distance for a region within a scene, many auto-focusing evaluation methods have been proposed to reduce the impact of DOF. The best focus plane can be determined by a maximum value of distribution curve along the optical axis through the light intensity of the particle center, the complex amplitude or the variance of imaginary part (Shen et al., 2005 and Ferraro et al., 2003). And these algorithms employ focus measures such as self-entropy (Gillespie et al., 1989), wavelet analysis (Liebling et al., 2004), the integrated amplitude modulus (Dubois et al., 2006), phase changes (Ma et al., 2004) and gray-level variance (Ferraro et al, 2003). But due to the impact of the depth of focus, these algorithms have property of less single-peak and poor stability.

In this paper, the mathematical formula of the DOF in the inline digital holographic system is derived and analyzed in detail with a new Fresnel number defined by the defocused parameter. Then in order to reduce the impact of DOF, an auto-focusing algorithm based on the most gradient for accurate location of particle was proposed. At the same time, another threshold parameter is introduced to improve the precision and stability of auto-focusing algorithm.

2. The influence of depth of focus for accurate axial location of particle

2.1 DOF of inline digital holographic system

According to the principle of holography, the hologram is recorded and reconstructed accurately only for a planar object. However, at certain conditions, a minute 3D object can be reconstructed with high accuracy. So the depth of focus of the digital holographic system can be defined the axial depth of the clearly reconstructed object. Although there is only the best clearly reconstructed object in theory, the defocused reconstructed object can be considered the same as the focused object within area of the DOF. Therefore, the DOF is an error of axial depth for clearly reconstructed object.

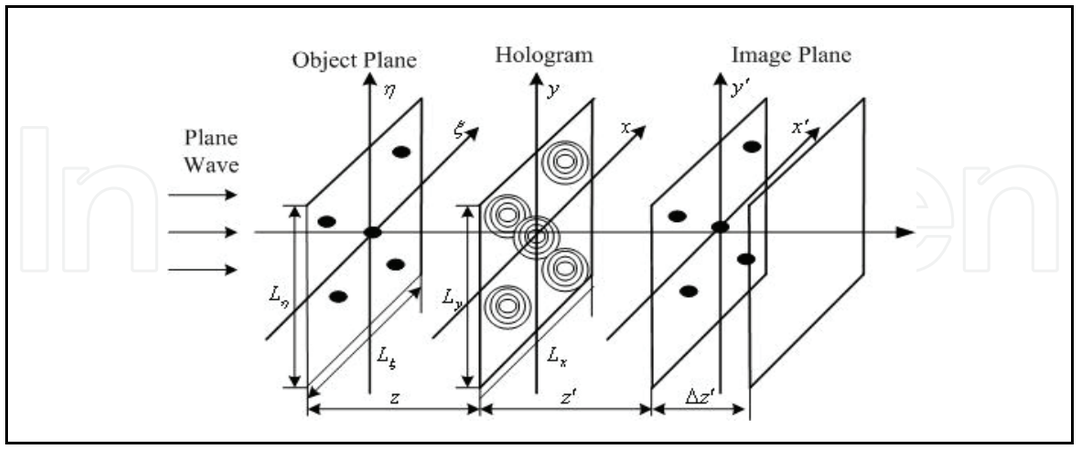

Fig. 1. Recording and reconstruction of in-line holography.

The particle hologram is recorded with the classical in-line holography arrangement. The principle of recording and reconstruction of hologram is shown in figure 1. Suppose that the monochromatic plane parallel wave of laser beam from left to right illuminate the particles on the object plane $\eta - \xi$, part of the wave is diffracted by particles and the remaining part

passes the setup without being diffracted saving as a reference wave, So we can have a hologram from CCD recording plane $x-y$ located at a distance z from the object plane on which the axisymmetric interference fringes for all the particles are recorded overlapping each other. The reconstructed particle image on image plane $x'-y'$ located at a distance z' from the hologram plane can be computed at the true depth where $z'=z$ to obtain the clearest image that is the shade of particle. In figure 1, L_x and L_y denote the length and width of CCD, L_ξ and L_η denote the length and width of particle field recorded. The distance $\Delta z'$ from the best clearly focus plane to actual image plane denotes the maximum axial depth which we can tolerant.

Now, taking the best focus plane as reference, i.e. $\frac{1}{z'}-\frac{1}{z}-\frac{1}{f}=0$, the defocus parameter $1/F$ can be expressed as following

$$\frac{1}{F}=\frac{1}{z'}-\frac{1}{z}-\frac{1}{f} \tag{1}$$

Because the particles are illuminated by plane wave in in-line holographic system without lens, as shown in figure 1, Eq. (1) can be written as

$$\frac{1}{F}=\frac{1}{z'}-\frac{1}{z} \tag{2}$$

where $1/F=0$ for perfectly focused image and $1/F\neq 0$ for defocused image. When $z'=z$, the perfectly focused image of particle can be obtained. Hence, the clearly reconstructed image of particle can be obtained from the location $z'=-z\pm\Delta z'$. So the expression of defocus parameter can be written as

$$\frac{1}{F}=\frac{1}{-z\pm\Delta z'}+\frac{1}{z}=\frac{\pm\Delta z'}{z(-z\pm\Delta z')} \tag{3}$$

A square aperture with a side length of L is assumed for the CCD. According to the definition of Fresnel number (Goodman, 2006), a new parameter N_F is defined as

$$N_F=\frac{W^2}{\lambda F} \tag{4}$$

where $W=\frac{L}{2}$.

In accordance with the definition of numerical aperture in traditional optical imaging system, if lens is not used in the digital holographic recording system and there exists a certain condition which meets $L<<z$, the numerical aperture NA of image system can be expressed as

$$NA=\frac{L}{2z}=\frac{W}{z} \tag{5}$$

From Eq. (4) and Eq. (5), Eq. (6) can be derived and written as

$$\frac{1}{F}=N_F\frac{\lambda}{z^2(NA)^2} \tag{6}$$

From Eq. (3), it is apparent that $\frac{z}{F} << 1$, in such a way that the Eq.(3) becomes

$$\mp\Delta z' \approx \frac{z^2}{F} = N_F \frac{\lambda}{(NA)^2} \tag{7}$$

The maximum axial depth which we can tolerant, that is depth of focus, can be expressed as

$$2\Delta z' = 2N_F \frac{\lambda}{(NA)^2} \tag{8}$$

In other words, Eq. (8) will determine the focus of depth for image system. As expected, the greater the numerical aperture of the system the shorter is focus of depth.

In inline digital holographic imaging system, the parameters λ and NA are known where NA can be calculated with the length L of CCD and recording distance z according to Eq. (5). Therefore, we can obtain the curve of the numerical relationship between $\Delta z'$ and $\lambda/(NA)^2$ under given conditions. The parameter N_F can be obtained by calculating the slope of the above line.

It is usual to regard a maximum loss of about 20% intensity as limit at the centre of the image of a point object, i.e. $I_{z'}(0,0) = 0.8I_z(0,0)$, is regarded as permissible for focused images, which is corresponding to $N_F = 0.5$. So the focus of depth can be written as

$$2\Delta z' = \frac{\lambda}{(NA)^2} \tag{13}$$

For visual detection the tolerance is more flexible. So the focus of depth will change with it.

2.2 The impact of depth of focus

From Eq. (8), the focus of depth in a in-line digital holographic system is mainly determined by the system parameters, the larger the numerical aperture of the system the shorter is focus of depth and the smaller the recording wavelength the shorter is focus of depth. Therefore, when the system parameters are fixed, we can shorten recording distance to increase the numerical aperture and reduce the DOF of system according to Eq. (5).

From the above analysis, we can see that the depth of focus significantly increases with recording distance. Generally, the depth of focus is tens of times or even hundreds of times more than particle diameter with tens of microns in in-line digital holographic system. So there are two adverse effects for the depth of focus to obtain precise axial location of particles. On the one hand, because within the depth of focus, all the reconstructed image of particle is clearer, it is very difficult to distinguish the clearest particle image. So the real axial location of particle is uncertain. It results lower measurement accuracy for the axial depth position of particle. Especially in DHPIV technology, the axial location of particle is key factors in analysis of velocity field. The impact of the DOF results in uncertainty and brings about larger errors. On the other hand, it is very important during the numerical reconstruction process. Because the reconstruction process is performed numerically, plane by plane to produce a region of the reconstructed volume, this is a very time-consuming process. With larger sampling interval, although the computational time can be reduced, if it is larger than the DOF, the real particle image may be “loss” and can not be reconstructed.

With smaller sampling interval, although real particle image can be reconstructed, the computational time will be increased significantly. Therefore, we must know the DOF to determine right sampling interval to locate all possible particles with less time before reconstructing particle fields.

3. General process for extracting 3D particle locations

Analyzing particle fields (such as velocity field computation from pairs of images and particle tracking in 3D turbulence flow) require a robust and accurate method for extracting particle coordinates from reconstructed 3D images. Our 3D particle field extraction process which consists of six different steps is shown in Fig.2. Here is a brief overview of the algorithm.

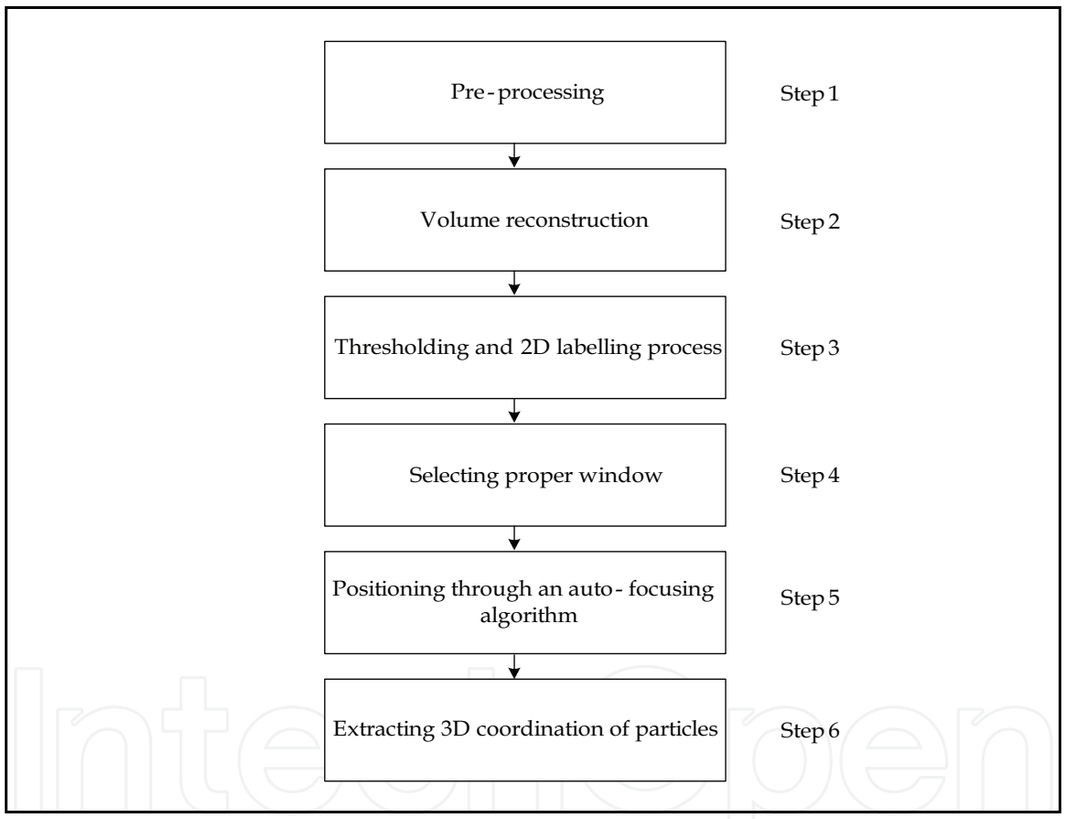

Fig. 2. General process for determining 3D particle locations

Step 1. The hologram of particles is pre-processed in this step to remove or suppress zero-order image from particle hologram by means of digital image processing technique, and to enhance the signal-to-noise ratio.

Step 2. The particle fields composed with amount of image slices are reconstructed from hologram at different depths. After reconstruction of each slice, median filtering is performed. Median filtering is effective in removing noise without disrupting edges, as long as the filter size is kept smaller than object feature sizes.

Step 3. This step is to identify the lateral position and size for particles in each depth by adaptive threshold. Then we will find all possible the centroids of particles. Note

that the lateral position and size of each window in reconstruction space varies depending on the reconstruction distance, growing larger and drifting farther from the optic axis as distance increases.

Step 4. Selecting proper window contains particle to be ready for digital image processing.

Step 5. An auto-focusing algorithm based on the most gradient for extracting particle axial position by selecting proper window in accordance with particle size is established. The focus measure is calculated for each window in each slice. For each window, the variation in the focus measure and irradiance over depth is analyzed. Hence, the axial depth of the particle in each window is determined. The variation of focus measure over depth is called the "focus curve." Note that the units are generally arbitrary, since the focus measure may not always have a direct physical significance.

Step 6. The final step is to extract 3D coordination of particles.

4. Auto-focusing algorithm for particle based on the most gradient

The particles that lie within the depth of focus of the imaging system are in focus (appearing sharp), while the particles that lie outside of the depth of field of the system are out of focus (appearing blurred). We now proceed to focus detection and demonstrate how, using a focus measure, we can determine the axial depth of particles in digital holographic reconstructions.

Focus measures are functions that attempt to determine the relative level of focus of sets of images. The accepted image property maximized by these functions is the high-spatial-frequency energy of the image. Hence, the edge of fully focused particle images has the larger gradient. So whether the particle is focused can be determined by calculating the edge gradient. Generally, the process for calculating the edge gradient of particles only calculates one or two gradient direction. However the real gradient direction for the edge of particle may not be the appointed direction, hence the gradients in all possible directions is calculated and chosen the largest gradient as the result.

To solve this problem, an auto-focusing algorithm based on the most gradient is proposed in this paper. First of all, the gradients in all possible directions is calculated in the focus window and chosen the largest gradient as the result. At the same time, taking into account the accuracy and the stability of algorithm, a threshold parameter which can effectively get rid of the background information and noise is introduced.

The edge gradient direction of a particle can only be in the horizontal direction, vertical direction, the 45 degree direction and negative 45 degree direction. In order to reduce the calculation error and obtain the real gradient direction, it is calculated as follows: the edge gradients in all directions are calculated in accordance with Formula (14) to (18) using any pixel including its eight surrounding pixels in focus window.

the edge of particle in horizontal direction (i=1)

$$\begin{cases} P1_i = f(x-1,y-1)+f(x-1,y)+f(x-1,y+1) \\ P2_i = f(x,y-1)+f(x,y)+f(x,y+1) \\ P3_i = f(x+1,y-1)+f(x+1,y)+f(x+1,y+1) \end{cases} \tag{14}$$

the edge of particle in vertical direction (i=2)

$$\begin{cases} P1_i = f(x-1,y+1) + f(x,y+1) + f(x+1,y+1) \\ P2_i = f(x-1,y) + f(x,y) + f(x+1,y) \\ P3_i = f(x-1,y-1) + f(x,y-1) + f(x+1,y) \end{cases} \tag{15}$$

the edge of particle in 45 degree direction (i=3)

$$\begin{cases} P1_i = f(x-1,y-1) + f(x-1,y) + f(x,y-1) \\ P2_i = f(x-1,y+1) + f(x,y) + f(x+1,y-1) \\ P3_i = f(x,y+1) + f(x+1,y) + f(x+1,y+1) \end{cases} \tag{16}$$

the edge of particle in -45 degree direction (i=4)

$$\begin{cases} P1_i = f(x-1,y) + f(x-1,y+1) + f(x,y+1) \\ P2_i = f(x-1,y-1) + f(x,y) + f(x+1,y+1) \\ P3_i = f(x,y-1) + f(x+1,y-1) + f(x+1,y) \end{cases} \tag{17}$$

$$\begin{cases} G1 = \left| P2_i - P1_i \right| \\ G2 = \left| P3_i - P2_i \right| \\ MAX_i = \max(G1,G2) \end{cases} \tag{18}$$

MAX1, MAX2, MAX3 and MAX4 are greater value in horizontal direction, vertical direction, the 45 degree direction and negative 45 degree direction. Because the real gradient direction can only be one of them, so a greater value in them can be selected as the real gradient direction. It is shown in Formula (19).

$$MAX = \max(MAX_1, MAX_2, MAX_3, MAX_4) \tag{19}$$

We can divide the focus window into several 3 × 3 windows to obtain real gradient value. However, due to the smaller 3 × 3 window, the result is noise-sensitive. In order to remove noise and reduce the impact of the background, a threshold having characterization of overall noise level distribution is defined as following

$$T = \sqrt{\frac{1}{M \times N} \sum_{x=0}^{M-1} \sum_{y=0}^{N-1} (f(x,y) - F_{mean})^2} \tag{20}$$

where M, N and F_{mean} denote the number of row and column and the mean value in focus window.

After T is calculated, then we can calculate the variance σ^2 of all 3×3 windows. Only if σ^2 is greater than T, the corresponding window maintains the gradient value, otherwise the gradient value is set to zero. The specific formula is as following

$$Gradient = \begin{cases} MAX^2 & \text{if} \quad \sigma^2 \geq T \\ 0 & \text{else} \end{cases} \tag{21}$$

The purpose for square of most gradient is to further enhance the effect of target image gradient values because the values of the edge gradient are always larger than the values of

non-edge gradient. Finally, the gradient values of each 3×3 window can be summed as the final gradient focusing value.

5. Results and discussion

The above extraction method has been tested using standard particles which is approximately parallel to the recording plane. The light source used is a He-Ne laser. The wavelength of the generated laser beam is $\lambda = 632.8$nm . The diffraction patterns are recorded by means of a CCD camera with 2032×1520 pixels of 6.4 mm×4.8mm.
Fig. 3 shows the axial location result of auto-focusing algorithm based on the most gradient for a particle with 500μm diameter which is recorded at 100mm. There are three auto-focusing curves under different sampling interval at 100μm, 500μm and 1000μm. As can be seen from the Fig. 3, the best focus plane of the particle can be determined by the maximum value of auto-focusing evaluation function. The auto-focusing curves based on the most gradient have the characteristics with better single peak feature, even when the sampling interval is 100μm. Auto-focusing algorithm has the same pulse width the sampling interval. There are no location errors.

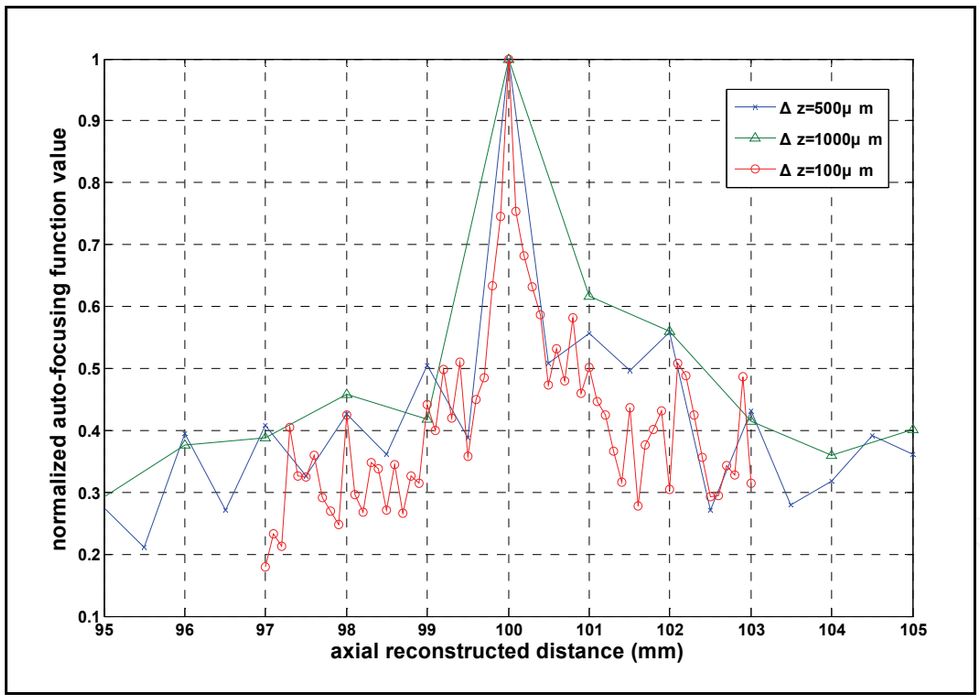

Fig. 3. Auto-focusing evaluation function based on the most gradient for a particle

Further two spherical particles with 500μm and 600μm diameter are selected as research objects. They are respectively located at 100mm and 105mm on sides of the optical glass. The results of auto-focusing function evaluation for two particles are shown in Fig.4. The axial sampling interval of auto-focusing curves is 500μm. As can be seen from the Fig.4, The auto-focusing curves based on the most gradient can accurately locate the axial depth position of two particles. Auto-focusing algorithm has the same pulse width the sampling interval. There are no location errors at 500μm sampling interval.

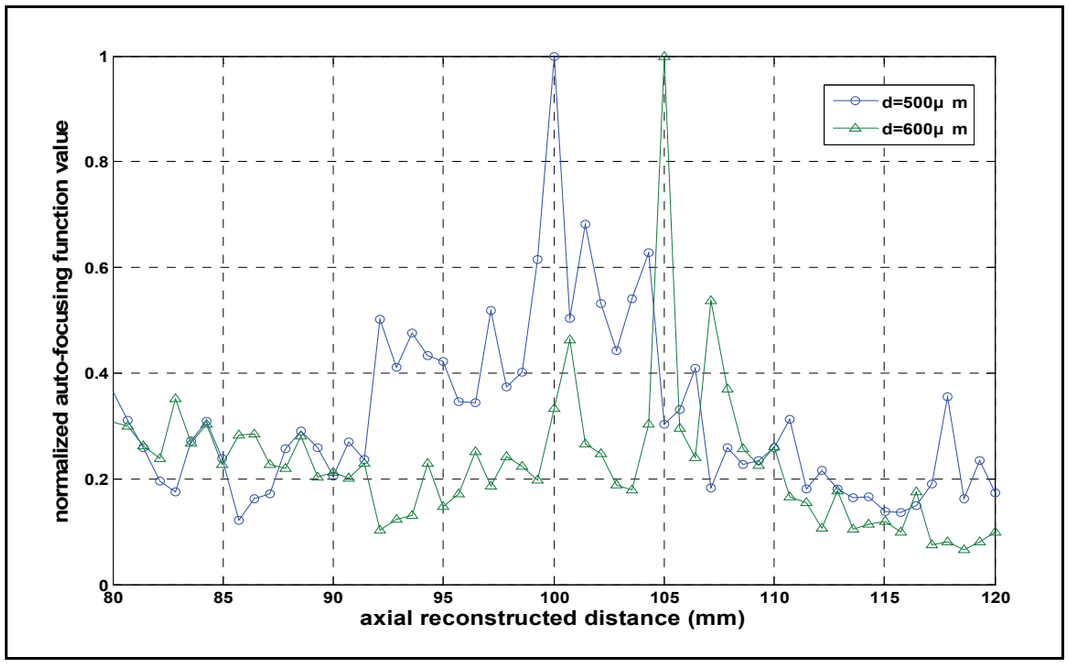

Fig. 4. Auto-focusing evaluation function based on the most gradient for two particles

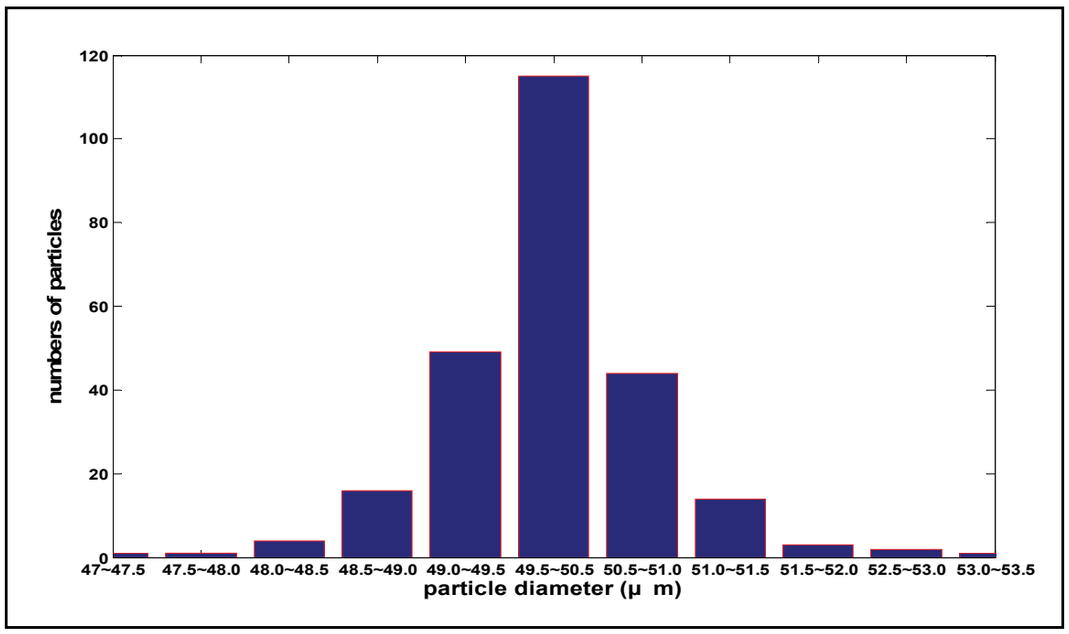

Fig. 5. The histogram of particles' diameter

To extract the particle field, we have built a sample volume corresponding to a set of reconstructed planes from 59.5mm to 60.5mm. The particle fields are consist of standard particles with 50μm diameter and 2 particles/mm3 concentration. Then, this volume has been processed according to the procedure discussed in Section 3. We have represented in Fig. 5 the histogram of the particles' diameter. This result is in good agreement with the standard particle distribution.

The above experimental study show that the axial locating errors mainly caused by larger depth of focus can be reduced by shortening the axial sampling interval and using auto-focusing algorithm based on the most gradient.

6. Conclusion

An auto-focusing algorithm based on the most gradient for extracting particle axial position by selecting proper window in accordance with particle size is established. This method provides a way of determining the depth of particles without prior knowledge of particle location. Using this algorithm, 3D coordination of particles can be extracted from the reconstructed volume. Taking into account the precision and stability of auto-focusing algorithm, another threshold parameter is introduced to remove noise and reduce the impact of the background. Experiment results show that the algorithm has the characteristics such as strong single peak feature and good stability.

7. Acknowledgment

This work was supported by Leading Academic Discipline Project of Shanghai Municipal Education Commission (Number: J51301) and the Program of Shanghai Municipal Education Commission under Grant (Number: 05LZ12)

8. References

Adams, M.; Kreis, T. & Jüptner, W. (2000). Particle analysis with digital holography. *Proceedings of SPIE*, pp. 314-320.

Dubois, F.; Schockaert, C.; Callens, N. & Yourassowsky, C. (2006). Focus plane detection criteria in digital holography microscopy. *Opt. Express* , Vol.14, 5895–5908.

Fournier, C.; Ducottet, C. & Fournel, T. (2004). Digital holographic particle image velocimetry: 3D velocity field extraction using correlation. Journal of Flow Visualization & Image Processing, Vol.11, pp. 53-72.

Ferraro, P.; Coppola, Nicola, G. Finizio, S. & Peirattini, G. (2003). Digital holographic microscope with automatic focus tracking by detecting sample displacement in real time. *Opt. Lett.* Vol.28, 1257–1259.

Gillespie, J.; King, R. (1989). The use of self-entropy as a focus measure in digital holography. *Pattern Recogn. Lett.* , Vol.9, 19–25.

GOODMAN, J. (2006). Introduction to Fourier optics. 3rd ed. Beijing: Publishing House of Electronics Industry, pp.141-143.

Kreis, T.; Jüptner, W. (1997). Suppression of DC term in digital holography. Optical Engineering, Vol. 36, No. 8, pp. 2357-2360.

Liebling, M.; Unser, M.. (2004). Autofocus for digital Fresnel holograms by use of a Fresnelet-sparsity criterion. *J. Opt. Soc. Am*. Vol. A21, 2424–2430.

Ma, L.; Wang, H.; Li,Y. & Jin, H. (2004). Numerical reconstruction of digital holograms for three-dimensional shape measurement. *J. Opt.*, Vol. A6, 396–400.

Meng, H.; Pan, G.; Pu, Y. et. al.. (2004). Holographic particle image velocimetry: from film to digital recording. *Meas. Sci. T*echnol., Vol. 15, pp.673-685.

Shen, G.; Wei, R. (2005). Digital holography particle image velocimetry for the measurement of 3Dt-3c flows. *Optics and Lasers in Engineering*, Vol. 43, pp. 1039-1055.

Takaki,Y.; Kawai, H. & Ohzu, H. (1999). Hybrid Holographic Microscopy Free of Conjugate and Zero-Order Images. *Applied Optics*, Vol. 38, No. 23, pp. 4990-4996.

Holography, Research and Technologies

Edited by Prof. Joseph Rosen

ISBN 978-953-307-227-2
Hard cover, 454 pages
Publisher InTech
Published online 28, February, 2011
Published in print edition February, 2011

Holography has recently become a field of much interest because of the many new applications implemented by various holographic techniques. This book is a collection of 22 excellent chapters written by various experts, and it covers various aspects of holography. The chapters of the book are organized in six sections, starting with theory, continuing with materials, techniques, applications as well as digital algorithms, and finally ending with non-optical holograms. The book contains recent outputs from researches belonging to different research groups worldwide, providing a rich diversity of approaches to the topic of holography.

InTech Europe
University Campus STeP Ri
Slavka Krautzeka 83/A
51000 Rijeka, Croatia
Phone: +385 (51) 770 447
Fax: +385 (51) 686 166
www.intechopen.com

InTech China
Unit 405, Office Block, Hotel Equatorial Shanghai
No.65, Yan An Road (West), Shanghai, 200040, China
中国上海市延安西路65号上海国际贵都大饭店办公楼405单元
Phone: +86-21-62489820
Fax: +86-21-62489821

IntechOpen